Nuclear localizations of Phosphatidylinositol-5-phosphate 4-kinases α and β are dynamic and independently regulated during starvation-induced stress.

Alaa Droubi[1]*, Simon J. Bulley[2]*, Jonathan H. Clarke & Robin F. Irvine[3]

Department of Pharmacology, University of Cambridge, Tennis Court Road, Cambridge, CB2 1PD. U.K.

* These authors contributed equally to this work.

1 Present address: Faculty of Life Sciences, University of Manchester, The Michael Smith Building, Oxford Road, Manchester, M13 9PT. U.K.

2 Present address: Department of Haematology, University of Cambridge School of Clinical Medicine, Cambridge Institute for Medical Research Wellcome Trust/MRC Building, Cambridge Biomedical Campus Box 139, Hills Road, Cambridge, CB2 0XY. U.K.

3 Corresponding author: rfi20@cam.ac.uk

Abstract

The chicken B-cell line DT40 has two isoforms of phosphatidylinositol 5-phosphate 4-kinase (PI5P4K), α and β, likely to exist as a mix of obligate homo- and hetero-dimers. Previous work has led us to speculate that an important role of the β isoform may be to target the more active PI5P4Kα isoform to the nucleus. Here we expand upon that work by genomically tagging the PI5P4Ks with fluorochromes in the presence or absence of stable or acute depletions of PI5P4Kβ. Consistent with our original hypothesis we find that PI5P4Kα is predominantly (possible entirely) cytoplasmic when PI5P4Kβ is stably deleted from cells. In contrast, when PI5P4Kβ is inducibly removed within an hour PI5P4Kα retains its wild type distribution of approximately 50:50 between cytoplasm and nucleus even through a number of cell divisions. This leads us to speculate that PI5P4Kα is chromatin associated. We also find that when cells are in the exponential phase of growth PI5P4Kβ is primarily cytoplasmic but translocates to the nucleus upon growth into the stationary phase or upon serum starvation. Once again this is not accompanied by a change in PI5P4Kα localization and we show, using an *in vitro* model, that this is possible because the dimerization between the two isoforms is dynamic. Given this shift in PI5P4Kβ upon nutrient deprivation we explore the phenotype of PI5P4Kβ null cells exposed to this stress and find that they can sustain a greater degree of nutrient deprivation than their wild type counterparts possibly as a result of upregulation of autophagy.

Summary Statement

It is presently believed that the phosphatidylinositol 5-phosphate 4-kinases are obligate dimers. Here we show that the isoforms can in fact be independently regulated which may account for the particular role of the beta isoform in stress responses including autophagy.

Short Title

Independent regulation of the phosphatidylinositol 5-phosphate 4-kinases.

Keywords

Phosphatidylinositol 5-phosphate 4-kinase; phosphatidylinositol 5-phosphate; starvation; autophagy; cell cycle.

Abbreviations

DNA	Deoxyribonucleic acid
EmGFP	Enhanced monomeric green fluorescent protein
FBS	Foetal bovine serum
PAGE	Polyacrylamide gel electrophoresis
PCR	Polymerase chain reaction
PI5P4K	Phosphatidylinositol 5-phosphate 4-kinase
PIP	Phosphatidylinositol phosphate
SDS	Sodium dodecyl sulphate

Introduction

The phosphatidylinositol 5-phosphate 4-kinases (PI5P4Ks) are a family of three (PI5P4Ks α, β and γ), whose cellular functions are still poorly understood (for reviews see [1-3]). Their principal activity is believed to be to remove, and thus regulate the levels of, their substrate PI5P, which is present in cells at slightly lower levels than PI3P and much lower levels than PI4P [1, 4]. PI5P has been reported to be present in the plasma membrane [4, 5], intracellular membranes [5] and the nucleus [6], and several studies suggest effectors and functions for this lipid in the nucleus [2, 7-9] and the cytoplasm [10].

The localization of the PI5P4Ks is clearly central to understanding their functions and those of PI5P, yet the literature has been confusing on this critical issue. Using immunolocalization of endogenous proteins, Boronenkov et al [11] reported that both PI5P4Kα and PI5P4Kβ were present in the nucleus, while transfection studies suggested that PI5P4Kα is primarily cytoplasmic and PI5P4Kβ is mostly nuclear with its localization being dictated by an unusual nuclear localization sequence, an α-helix [12] numbered α-7 in the structure of PI5P4Kβ [13]. However, using highly isoform-specific antibodies, Bultsma et al [14] reported that both PI5P4Kα and PI5P4Kβ were in the nucleus and cytoplasm, while using genomic tagging of PI5P4Ks in DT40 cells Richardson et al [15] and Wang et al [16] reported that PI5P4Kβ was almost entirely nuclear while PI5P4Kα was 40% nuclear and 60% cytoplasmic.

A complicating factor in understanding these issues has been the discovery that PI5P4Kα and PI5P4Kβ heterodimerize [14, 16] as might be expected given that their dimerization sequences [13] are near identical between the isoforms. Indeed Bultsma et al showed that PI5P4Kα and PI5P4Kβ are likely to exist as a mix of obligate homo and heterodimers *in vivo* [14]. DT40 cells, being of avian origin, lack a PI5P4Kγ isoform [16, 17], but we have shown that PI5P4Ks α and γ can also heterodimerize at least *in vitro* [17], so there is no reason to suppose that PI5P4Kβ and PI5P4Kγ will not heterodimerize too. So two key questions concerning PI5P4K and PI5P functions in the nucleus are: is PI5P4Kβ cytoplasmic [14] because it is pulled out of the nucleus by one or both of the other isoforms, and is a primary role of PI5P4Kβ to target the much more enzymatically active PI5P4Kα [14, 16] to the nucleus [16]?

To resolve these issues we have further employed the remarkable genetic power of DT40 cells to tag both the endogenous PI5P4Ks with EmGFP, to delete both alleles of PI5P4Kβ, and to tag both alleles of PI5P4Kβ with the auxin degron [18] so that we can remove it from the cells within minutes. In all cases we can follow the localization of the endogenous proteins by cell fractionation or confocal imaging, and by these strategies we have gained significant insight into the dynamic relationship between these two proteins.

Materials and Methods

DT40 tissue culture

Basic culture medium for DT40 cells was formulated according to the protocol of [23]. To 500ml of RPMI medium was added 50ml of FBS,
5ml of 200mM L-glutamine, 5ml of chicken serum, and 120**µ**l of 50mM 2-mercaptoethanol. Cells were cultured at 41°C in 5% carbon dioxide.

Generation of targeting constructs for targeted transfection of DT40 cells

Targeting constructs were built into an appropriate plasmid vector (typically pBluescript SK+ (Stratagene)). For gene deletions sequences of genomic DNA flanking the region to be deleted (targeting arms) were PCR amplified from DT40 genomic DNA and ligated into the plasmid vector separated by an antibiotic resistance cassette to allow selection of drug-resistant clones. The targeting arms were

typically 2kb in length. Following successful transfection and integration into the germline by homologous recombination the antibiotic resistance cassette replaced the region of the gene targeted for deletion. For integration of tags into the germline a similar strategy was employed, but in this case the targeting arms were manipulated such that successful recombination led to introduction of the new sequence of choice. See supplementary methods for further details.

Targeted transfection of DT40 cells

Targeting constructs were linearized using an appropriate restriction enzyme, recovered by lithium chloride precipitation, and transfected into DT40 cells in the logarithmic phase of growth by electroporation (600V, 25**µ**F, exponential pulse, Biorad Gene Pulser XCell). The cells were then immediately seeded out in 96 well plates and 24 hours later the appropriate selection antibiotic(s) was added. Colonies resulting from single cells were picked and subjected to sequencing in order to verify correct construct integration. All results were verified in multiple independently derived clones.

Fractionation of nuclear and cytoplasmic proteins in DT40 cells

This was performed essentially as set out in [23]. $1x10^7$ cells were harvested by centrifugation at 300g for 5 mins and washed twice in PBS before being resuspended in 1ml of suspension buffer (0.32M sucrose and protease inhibitor cocktail in PBS). 10µl of 10% (v/v) IGEPAL CA-630 in PBS was added to the cell suspension with mixing by gentle pipetting to give a final detergent concentration of 0.1%. The suspension was immediately centrifuged at 5500rpm for 30 secs at 4°C in a microcentrifuge to pellet the nuclei. The supernatant was aspirated and kept as the cytoplasmic protein fraction. The nuclei were resuspended in 1ml of suspension buffer to wash them. Prior to centrifugation at 1500rpm for 5 mins at 4°C an aliquot was examined by light microscopy to check that the nuclei were clean. The nuclear pellet was next resuspended in 1ml of nuclear extraction buffer (20mM HEPES pH 7.7, 1.5mM magnesium chloride, 0.42M sodium chloride, and protease inhibitor cocktail in water) and incubated on ice for 20 minutes. This suspension was then centrifuged at 9400rpm for 15 mins at 4°C in a microcentrifuge and the supernatant aspirated as the nuclear protein fraction. In all fractionation experiments the protein species being examined was immunoprecipitated from the fractions before being

blotted. We always used an excess of immunoprecipitating antibody and so all the protein we could recover from the fractions is loaded onto the gel.

Immunoprecipitation of proteins from DT40 cells

The antibody for immunoprecipitation was conjugated to protein G sepharose beads which were then used to immunoprecipitate the target protein from cell free extract. An excess of antibody over antigen was used as determined empirically. Antigen was eluted from the beads by boiling in SDS loading buffer in preparation for denaturing polyacrylamide gel electrophoresis.

Western blotting

Following denaturing SDS-PAGE electrophoresis proteins were transferred onto an appropriate blotting membrane, which was probed with antibodies as detailed in the supplementary methods and detected using chemiluminescent reagent of an appropriate sensitivity.

Confocal Microscopy

Images were acquired with a Leica SP5 confocal microscope attached to a Leica DMI6000 inverted microscope stand. For GFP imaging excitation was with the 488nm line of the argon laser and emission was detected between 500 and 550nm. For all imaging the confocal pinhole was set to 1 Airy unit, and an oil immersion 40x 1.25 NA objective lens was used. All imaging was performed on live cells, which were embedded in Matrigel to prevent cell movement and transferred to uncoated glass bottom MatTek dishes. Just prior to imaging full growth medium was removed and replaced with RPMI without phenol red. Imaging was performed at 41°C under 5% CO2.

Dimerization assays

Untagged recombinant PI5P4Kγ was allowed to reach equilibrium at a concentration where dimers were the predominant form [17] and then diluted to a concentration where we would expect dissociation into monomers [17]. Samples of this solution were then taken every 5 to 15 minutes to monitor the kinetics of dimer dissociation. These samples were cross-linked within 1 second (not shown) with a 50 fold molar excess of BS3 [bis(sulfosuccinimidyl)suberate] and the reaction was quenched with

50mM Tris/HCl, pH 7.4. The mixture of dimers and monomers present was assayed by denaturing SDS-PAGE followed by western blotting with an anti-PI5P4Kγ antibody (see supplementary methods).

Cell cycle analysis by flow cytometry

$1x10^7$ cells were fixed in ethanol then stained with 25 micrograms/ml propidium iodide containing RNaseA at 250 micrograms/ml. Cells were analysed using a BD FACScan, exciting with the 488nm line of the argon laser and collecting through the 650nm long-pass filter. Dead cells were excluded as were cellular doublets and higher order clumps. At least $1x10^5$ events were collected for each sample.

Results and Discussion

PI5P4Kα is almost exclusively cytoplasmic upon genetic deletion of *PIP4K2B*

If our speculation based upon previous data [16] is correct that PI5P4Kα requires targeting by PI5P4Kβ to enter the nucleus then we reasoned that PI5P4Kα should be exclusively cytoplasmic in *PIP4K2B* null cells. We therefore created a cell line in which both alleles of *PIP4K2B* were deleted and one allele of *PIP4K2A* was endogenously tagged at the C-terminus with the coding sequence for EmGFP ($PIP4K2A^{EmGFP/wt/wt}$ $PIP4K2B^{-/-}$ cells). Note that karyotype analysis shows DT40 cells exhibit trisomy for chromosome 2, the chromosome on which the *PIP4K2A* gene is located (not shown). $PIP4K2A^{EmGFP/wt/wt}$ cells (with wild type *PIP4K2B*) acted as a control. As anticipated [16] PI5P4Kα is distributed approximately equally between cytoplasm and nucleus in a wild type *PIP4K2B* background whilst deletion of *PIP4K2B* results in a marked shift of PI5P4Kα out of the nucleus (figure 1A and B). It is impossible to know whether the small amount of PI5P4Kα that persists in the nuclear fraction in *PIP4K2B* null cells is truly nuclear or whether this represents an artifact of an inevitably less than perfect separation of nucleus from cytoplasm. Certainly no nuclear PI5P4Kα-EmGFP is visible in the nuclei of these cells upon confocal microscopy (not shown) although this is a less sensitive technique than immunoprecipitation and western blotting and so does not really help to answer the question. Whatever the truth of the matter it is certainly accurate to say that genomic deletion of *PIP4K2B* results in PI5P4Kα distributing away from the nucleus largely, possibly entirely. It is, of course, important to know that endogenous tagging does not

affect protein function, and we address this further under supplementary results and discussion.

Acute depletion of PI5P4Kβ does not result in any redistribution of PI5P4Kα

In light of these findings we thought it would be interesting to study the kinetics of redistribution of PI5P4Kα away from the nucleus upon acute removal of PI5P4Kβ. We therefore created a cell line in which PI5P4Kβ was endogenously tagged (at both alleles) with the auxin degron system [18] in order to enable the localization of PI5P4Kα endogenously tagged with EmGFP to be studied upon rapid depletion of PI5P4Kβ by addition of auxin. Note that we placed a $(His)_6$-FLAG tag in frame with the degron tag on the *PIP4K2B* alleles to allow for easy immunoprecipitation and blotting of the fusion protein. The resultant cell line is $PIP4K2A^{EmGFP/wt/wt}PIP4K2B^{degron/degron}$. To our surprise removal of PI5P4Kβ, which as far as we can tell from immunoprecipitation and western blotting is (virtually) complete (figure 2A), has no effect on the localization of PI5P4Kα which remains approximately equally distributed between the cytoplasm and nucleus (figure 2B). This persists even after 16 hours of PI5P4Kβ depletion by which time these rapidly proliferating cells have gone through two or three rounds of division with breakdown and re-formation of the nuclear envelope. This makes unlikely the explanation that PI5P4Kα has simply been 'ferried' to the nucleus by PI5P4Kβ where it becomes trapped by the nuclear envelope, but coupled with the requirement PI5P4Kα has for PI5P4Kβ to enter the nucleus in the long-term (figure 1A,B) it is possible that nuclear PI5P4Kα is chromatin associated. Unfortunately problems with auxin toxicity after about 24 hours mean we are unable to continue PI5P4Kβ depletion for long enough to observe the 'acute' phenotype transform into the 'chronic' phenotype.

In these cells we also took the opportunity to study the distribution of degron tagged PI5P4Kβ between cytoplasm and nucleus. To our surprise PI5P4Kβ was predominantly (about 90%) cytoplasmic (figure 2B). This is in complete contradiction to our previous data where PI5P4Kβ endogenously tagged with $(His)_6$-FLAG was found to be 90% nuclear [16]. In order to confirm this finding and convince ourselves that everything we found with the degron system was not artefactual, we decided to re-explore the entire issue of the localization of PI5P4Kα and PI5P4Kβ using

endogenous EmGFP tags in an otherwise wild-type background, particularly as we have data elsewhere (Bulley, Droubi *et al.,* unpublished) demonstrating that endogenous EmGFP tags do not affect the *in vivo* function, and therefore presumably localization, of the PI5P4Ks. Note that we have already presented data from PIP4K2A$^{EmGFP/wt/wt}$ cells (figure 1A) but we decided to go on to tag a second *PIP4K2A* allele with EmGFP in order to enhance the signal for confocal microscopy.

Localization of EmGFP-tagged PI5P4Kα and PI5P4Kβ

Once again we used the high homologous recombination frequency of the DT40 line to knock EmGFP tags into two *PIP4K2A* alleles and both *PIP4K2B* alleles in separate cells lines to create PIP4K2A$^{EmGFP/EmGFP/wt}$ and PIP4K2B$^{EmGFP/EmGFP}$ cells respectively. We looked at the localization of the tagged proteins by both confocal microscopy and cell fractionation. As expected PI5P4Kα has an approximately equal cytoplasmic / nuclear localization (figure 3A,B) (cytoplasm to nuclear ratio 1.2, 95% CI 1.1 to 1.3, n=3), which is consistent with what we have seen throughout this current study, and consistent with what we have reported before in these cells [16] and what others have reported for the endogenous protein in mammalian cells [11, 14].

PI5P4Kβ, in contrast, is almost entirely cytoplasmic (figure 3A,B) (cytoplasm to nuclear ratio 11.5, 95% CI 8.2 to 14.7, n=3). Whilst this is consistent with what we saw with degron-tagged PI5P4Kβ (above) it is completely inconsistent with what we previously reported in DT40s [15, 16] where we found PI5P4Kβ to be almost exclusively nuclear upon both overexpression and endogenous tagging, and indeed inconsistent with most reports on other cells [11, 14]. We wondered if this inconsistency was a result of the different growth state of the cells, as in the present experiments we were careful to assay the cells in the exponential phase of growth, whereas in our earlier experiments [16] we had grown the cells into or close to the stationary phase in order to get the maximum yield of protein for downstream applications. We therefore let the cells grow on into the stationary phase and an almost complete shift in PI5P4Kβ towards the nuclear compartment was revealed (figure 4A), making the present results consistent with our earlier study [16] as long as the cells are sampled under the correct experimental conditions. Live cell confocal

microscopy reveals that translocation of PI5P4Kβ to the nucleus upon growth into the stationary phase occurs in some cells before others (figure 4C left panel). We confirmed this result in the cells we have already described (figure 2) in which PI5P4Kβ is tagged at both alleles with the auxin degron and $(His)_6$-FLAG (figure 4B). Once again acute removal of PI5P4Kβ by addition of auxin resulted in no change in the subcellular localization of PI5P4Kα (figure 4B). To investigate what the major factor might be in causing this change we transferred PIP4K2B$^{EmGFP/EmGFP}$ cells in the logarithmic phase of growth to a medium with no soluble nutrients (amino acids etc), or to one with no added serum. The former caused no change (not shown), but in cells deprived of serum a translocation of PI5P4Kβ to the nucleus occurred within an hour (figure 4D). Finally, we repeated these experiments with PIP4K2A$^{EmGFP/EmGFP/wt}$ cells, and saw no significant change in PI5P4Kα localization, either growing the cells into the stationary phase (not shown) or depriving them of serum (figure 4D).

Kinetics of dimer dissociation

In the context of seemingly independent behaviour of PI5P4Kα and PI5P4Kβ under conditions of serum deprivation and acute depletion of PI5P4Kβ it is relevant to remember that the two PI5P4K isoforms are extensively heterodimerizing in DT40 cells [16]. So the independent movement of PI5P4Kβ into the nucleus while PI5P4Kα remains apparently unmoved (figure 4D), plus the unchanged location of PI5P4Kα while PI5P4Kβ is removed, both suggest that the two PI5P4Ks are in quite a rapid equilibrium; these observations would be inconsistent with a stable heterodimerization where once bound to each other the two remained so over a long time course. However, we currently have no idea at all what the likely timescale of their binding to each other is. But we can address this question indirectly by exploring the dissociation of PI5P4Kγ homodimers.

We used this surrogate strategy for three reasons: Firstly, because it is essential that we should use untagged protein (tags might enhance or hinder the interaction) and we do not have the necessary isoform-specific antibodies for PI5P4Kα and PI5P4Kβ, whereas we do have an anti-PI5P4Kγ antibody [19]; secondly, creating and isolating a pure PI5P4Kα/PI5P4Kβ heterodimer population to investigate dissociation would be extremely difficult; and thirdly, the hydrogen bonding between PI5P4Kγ homodimers

is almost exactly the same as PI5P4Kα/PI5P4Kβ heterodimers [17], so PI5P4Kγ homodimers are a suitable model to investigate this question.

Figure 5 shows a typical experiment where we incubated recombinant PI5P4Kγ at a concentration at which it is dimeric [17], and then diluted rapidly to a concentration at which it is entirely monomers [17], taking samples every 5-15 minutes and adding a cross-linker at a concentration that stabilized the dimers within 1 second (not shown). Because our antibody does not immunoprecipitate we could not easily concentrate the diluted enzyme before gel electrophoresis and western blotting, so detection and quantification of the extremely dilute protein preparations pushes the sensitivity of western blotting to the extreme. But it is nevertheless clear even from this semi-quantitative experiment (figure 5) that the dissociation of the PI5P4Kγ dimers is detectable within a few minutes with an approximate half life of 10-15 mins. This short time frame is consistent with the independent behaviour of PI5P4Ks α and β in the contexts discussed above.

PIP4K2B$^{-/-}$ cells are able to sustain high levels of nutrient deprivation

Given the nuclear translocation of PI5P4Kβ upon proliferation of cells into the stationary phase we wondered whether the growth characteristics of *PIP4K2B* knockout cells would differ from those of their wild type counterparts. As a control we generated *PIP4K2A* null cells (PIP4K2A$^{-/-/-}$). Consistent with the subcellular localization data the growth characteristics of PIP4K2A$^{-/-/-}$ cells are unchanged compared to wild type (data not shown) but PIP4K2B$^{-/-}$ cells remain in the exponential phase of growth for longer than their wild type controls. This results in PIP4K2B$^{-/-}$ cells attaining a higher cell density in the plateau phase than wild type DT40 cells (figure 6A). This difference in growth characteristics is interesting, particularly since the type 1 and type 2 PIP kinases can interact [20], and the type 1 PtdInsP kinases in turn interact with the G1/S checkpoint protein retinoblastoma [21]. We therefore wondered whether loss of *PIP4K2B* resulted in dysregulation of the G1/S checkpoint. Cell cycle analysis by flow cytometry shows that PIP4K2B$^{-/-}$ cells continue to proliferate for longer than wild type (which we knew anyway from the growth curves) but following this extended period of growth they do enforce the G1/S checkpoint appropriately (figure 6B).

Autophagy is upregulated in PIP4K2B$^{-/-}$ cells

Given that the outgrowth of PIP4K2B-/- cells does not seem to be due to breakdown of the G1/S checkpoint we wondered whether autophagy, a mechanism for promoting cellular survival during periods of starvation [22], might be affected. We therefore assayed autophagy by blotting against the autophagy marker LC3-II, and found that autophagy is enhanced in PIP4K2B$^{-/-}$ cells (figure 7A) but not in PIP4K2A$^{-/-/-}$ cells (not shown). The best characterized regulator of autophagy is mTORC1, which acts as a negative regulator [22]. We therefore hypothesized that mTORC1 would be less active in PIP4K2B$^{-/-}$ cells (but not in PIP4K2A$^{-/-/-}$ cells) and indeed find this to be the case by blotting for phosphorylation of the mTORC1 target p70S6K (figure 7B). We have data elsewhere (Bulley, Droubi *et al.,* in submission) showing that loss of PI5P4Kβ does not affect Akt phosphorylation and so the influence of PI5P4Kβ does not appear to extend to mTORC2 targets. It may therefore be that PI5P4Kβ regulates autophagy via a direct or indirect impact upon mTORC1 activity. It was recently suggested that knockdown of any of the three mammalian isoforms of PI5P4K can induce autophagy due to build up of their substrate PI5P which in turn recruits autophagy effectors normally held to be dependent upon PI3P [24]. Our data is not entirely consistent with this but investigation of the mechanism linking PI5P4Kβ to autophagy may be an interesting and fruitful avenue for future work.

Acknowledgements

A.D. was supported by Sidney Sussex College, the Cambridge Overseas Trusts and the Säid Foundation, S.J.B. by an A.J. Clarke Studentship of the British Pharmacological Society and J.H.C. by the MRC (Grant RG64071). We thank Ashok Venkitaraman and Gerard Evan for the kind gifts of reagents.

Declarations of Interest

None.

Funding Information

This work was funded by MRC Grant RG64071 (to R.F.I.) and by a British Pharmacological Society A.J. Clark Studentship (to S.J.B. and R.F.I.).

Author Contribution Statement

A.D., S.J.B., J.H.C. and R.F.I. designed and performed the experiments.

S.J.B. and R.F.I. wrote the paper.

References

1 Balla, T. (2013) Phosphoinositides: tiny lipids with giant impact on cell regulation. Physiol Rev. **93**, 1019-1137

2 Viaud, J., Boal, F., Tronchere, H., Gaits-Iacovoni, F. and Payrastre, B. (2014) Phosphatidylinositol 5-phosphate: a nuclear stress lipid and a tuner of membranes and cytoskeleton dynamics. BioEssays : news and reviews in molecular, cellular and developmental biology. **36**, 260-272

3 Bulley, S. J., Clarke, J. H., Droubi, A., Giudici, M. L. and Irvine, R. F. (2015) Exploring phosphatidylinositol 5-phosphate 4-kinase function. Advances in biological regulation. **57**, 193-202

4 Roberts, H. F., Clarke, J. H., Letcher, A. J. and Irvine, R. F. (2005) Effect of lipid kinase expression and cellular stimuli on phosphatidylinositol 5-phosphate levels in mammalin cell lines. FEBS Lett. **579**, 2868-2872

5 Sarkes, D. and Rameh, L. E. (2010) A novel HPLC-based approach makes possible the spatial characterization of cellular PtdIns5P and other phosphoinositides. Biochem. J. **428**, 375-384

6 Clarke, J. H., Letcher, A. J., S., D. C., Halstead, J. R., Irvine, R. F. and Divecha, N. (2001) Inositol lipids are regulated during cell cycle progression in the nuclei of murine erythroleukaemia cells. Biochem. J. **357**, 905-910.

7 Jones, D. R., Bultsma, Y., Keune, W. J., Halstead, J. R., Elouarrat, D., Mohammed, S., Heck, A. J., D'Santos, C. S. and Divecha, N. (2006) Nuclear PtdIns5P as a Transducer of Stress Signaling: An In Vivo Role for PIP4Kbeta. Mol. Cell. **23**, 685-695

8 Keune, W. J., Jones, D. R., Bultsma, Y., Sommer, L., Zhou, X. Z., Lu, K. P. and Divecha, N. (2012) Regulation of phosphatidylinositol-5-phosphate signaling by Pin1 determines sensitivity to oxidative stress. Science signaling. **5**, ra86

9 Shah, Z. H., Jones, D. R., Sommer, L., Foulger, R., Bultsma, Y., D'Santos, C. and Divecha, N. (2013) Nuclear phosphoinositides and their impact on nuclear functions. The FEBS journal. **280**, 6295-6310

10 Boal, F., Mansour, R., Gayral, M., Saland, E., Chicanne, G., Xuereb, J. M., Marcellin, M., Burlet-Schiltz, O., Sansonetti, P. J., Payrastre, B. and Tronchere, H. (2015) TOM1 is a PI5P effector involved in the regulation of endosomal maturation. J Cell Sci. **128**, 815-827

11 Boronenkov, I. V., Loijens, J. C., Umeda, M. and Anderson, R. A. (1998) Phosphoinositide signaling pathways in nuclei are associated with nuclear speckles containing pre-mRNA processing factors. Mol. Biol. Cell. **9**, 3547-3560

12 Ciruela, A., Hinchliffe, K. A., Divecha, N. and Irvine, R. F. (2000) Nuclear targeting of the β isoform of Type II phosphatidylinositol phosphate kinase (phosphatidylinositol 5-phosphate 4-kinase) by its α-helix 7. Biochem. J. **364**, 587-591

13 Rao, V. D., Misra, S., Boronenkov, I. V., Anderson, R. A. and Hurley, J. H. (1998) Structure of type IIbeta phosphatidylinositol phosphate kinase: a protein kinase fold flattened for interfacial phosphorylation. Cell. **94**, 829-839

14 Bultsma, Y., Keune, W. J. and Divecha, N. (2010) PIP4Kβ interacts with and modulates nuclear localisation of the high activity PtdIns5P-4-kinase isoform, PIP4Kα. Biochem. J. **430**, 223-235

15 Richardson, J. P., Wang, M., Clarke, J. H., Patel, K. J. and Irvine, R. F. (2007) Genomic tagging of endogenous type IIbeta phosphatidylinositol 5-phosphate 4-kinase in DT40 cells reveals a nuclear localisation. Cell Signal. **19**, 1309-1314

16 Wang, M., Bond, N. J., Letcher, A. J., Richardson, J. P., Lilley, K. S., Irvine, R. F. and Clarke, J. H. (2010) Genomic tagging reveals a random association of endogenous PtdIns5P 4-kinases IIα and IIβ and a partial nuclear localisation of the IIα isoform. Biochem. J. **430**, 215-221

17 Clarke, J. H. and Irvine, R. F. (2013) Evolutionarily conserved structural changes in phosphatidylinositol 5-phosphate 4-kinase (PI5P4K) isoforms are responsible for differences in enzyme activity and localization. Biochem J. **454**, 49-57

18 Nishimura, K., Fukagawa, T., Takisawa, H., Kakimoto, T. and Kanemaki, M. (2009) An auxin-based degron system for the rapid depletion of proteins in nonplant cells. Nat. Methods. **6**, 917-922

19 Clarke, J. H., Emson, P. C. and Irvine, R. F. (2008) Localization of phosphatidylinositol phosphate kinase IIgamma in kidney to a membrane trafficking

compartment within specialized cells of the nephron. Am. J. Physiol. Renal Physiol. **295**, F1422-1430

20 Hinchliffe, K.A., Giudici, M.L., Letcher, A.J. and Irvine, R.F. (2002) Type IIalpha phosphatidylinositol phosphate kinase associates with the plasma membrane via interaction with type I isoforms. Biochem. J. **363,** 563-570

21 Divecha, N., Roefs, M., Los, A., Halstead, J., Bannister, A. and D'Santos, C. (2002) Type I PIPkinases interact with and are regulated by the retinoblastoma susceptibility gene product-pRB. Current Biology **12,** 582-587

22 Lamb, C.A., Yoshimori, T. and Tooze, S.A. (2013) The autophagosome: origins unknown, biogenesis complex. Nat. Rev. Mol. cell biol. **14,** 759-774

23 Buerstedde, J.M. and Takeda, S. (Eds.) (2006) Reviews and Protocols in DT40 Research. New York: Springer

24 Vicinanza, M., Korolchuk, V.I., Ashkenazi, A., Puri, C., Menzies, F.M., Clarke, J.H. and Rubinsztein, D.C. (2015) PI(5)P regulates autophagosome biogenesis. Mol. Cell. **57,** 219-234.

Figure Legends

Figure 1

Effect of deletion of *PIP4K2B* on the cellular localization of PI5P4Kα. The PI5P4Kα-EmGFP fusion protein was detected by immunoprecipitation and blotting against the EmGFP tag. 10^7 cells were fractionated into cytoplasmic and nuclear fractions and the EmGFP fusion protein was recovered from the fractions with an excess of immunoprecipitating antibody.

A: Distribution of PI5P4Kα between cytoplasm and nucleus in cells with either wild type or deleted *PIP4K2B*. β-actin and histone H3 blots are shown as fractionation markers. Immunoprecipitation with Invitrogen A-6455 anti-GFP and blots with Invitrogen 33-2600 anti-GFP, Sigma AC74 anti-beta actin, and Abcam ab1791 anti-histone H3.

B: Quantification of three such blots by densitometry. Bars shows mean and 95% confidence interval.

Figure 2

Effect of acute removal of PI5P4Kβ on the cellular localization of PI5P4Kα. The PI5P4Kβ-degron fusion protein was detected by immunoprecipitation against the FLAG epitope and blotting against the poly-His tag. PI5P4Kα was detected as described for figure 1. Auxin was used at a concentration of 500 micromolar.

A: Treatment of $PIP4K2B^{degron/degron}$ cells with auxin for 30 minutes renders PI5P4Kβ undetectable. Immunoprecipitation with Sigma A2220 anti-FLAG and blot with Abcam ab9108 anti-hexaHis.

B: Distribution of PI5P4Kα and PI5P4Kβ between cytoplasm and nulceus with no auxin treatment, or auxin treatment for 4 or 16 hours. We do not know the identity of the non-specific band in the cytoplasmic fractions. Cytoplasmic and nuclear fractions were assessed as adequately pure (data not shown) in the same way as in figure 1. 10^7 cells were fractionated into cytoplasmic and nuclear fractions and the fusion protein was recovered from the fractions with an excess of immunoprecipitating antibody. Immunoprecipitation with Invitrogen A-6455 anti-GFP or Sigma A2220 anti-FLAG and blots with Invitrogen 33-2600 anti-GFP or Abcam ab9108 anti-hexaHis. Representative blot from three biological replicates.

Figure 3

Cellular localization of PI5P4Kα and PI5P4Kβ with genomic EmGFP tags in DT40 cells. The fusion proteins were detected as described for figure 1.

A: Distribution of the PI5P4Ks between cytoplasm and nucleus in cells in the logarithmic phase of growth. Cytoplasmic and nuclear fractions were assessed as adequately pure (data not shown) in the same way as in figure 1. 10^7 cells were fractionated into cytoplasmic and nuclear fractions and the EmGFP fusion protein was recovered from the fractions with an excess of immunoprecipitating antibody. Immunoprecipitation with Invitrogen A-6455 anti-GFP and blot with Invitrogen 33-2600 anti-GFP.

B: Live cell confocal images of the same cell lines.

Figure 4

Nuclear translocation of PI5P4Kβ upon cell growth into the stationary phase or serum starvation. The EmGFP and degron containing fusion proteins were detected as described for figures 1 and 2 respectively. Cytoplasmic and nuclear fractions were assessed as adequately pure (data not shown) in the same way as in figure 1. 10^7 cells were fractionated into cytoplasmic and nuclear fractions and the fusion protein was recovered from the fractions with an excess of immunoprecipitating antibody.

A: Distribution of PI5P4Kβ between cytoplasm and nucleus as cells move from the logarithmic to stationary phase of growth. Immunoprecipitation with Invitrogen A-6455 anti-GFP and blot with Invitrogen 33-2600 anti-GFP. Representative blot from three biological replicates.

B: Distribution of the PI5P4Kβ-degron fusion protein between cytoplasm and nucleus when cells are in the stationary phase of growth, and the effect of auxin treatment upon PI5P4Kα localization. Top blot shows the PI5P4Kβ-degron fusion protein. Bottom blot shows the PI5P4Kα-EmGFP fusion protein. Auxin was used at a concentration of 500 micromolar. Immunoprecipitation with Invitrogen A-6455 anti-GFP or Sigma A2220 anti-FLAG and blots with Invitrogen 33-2600 anti-GFP or Abcam Ab9108 anti-hexaHis. Representative blot from three biological replicates.

C: Live cell confocal images of $PIP4K2B^{EmGFP/EmGFP}$ cells as they enter the stationary phase of growth. Scale bars represent 10 micrometres.

D: Distribution of PI5P4Kα and PI5P4Kβ between cytoplasm and nucleus when cells are serum replete in the logarithmic phase of growth, and when they are switched to serum free medium for 1 hour whilst in the logarithmic phase of growth. Immunoprecipitation with Invitrogen A-6455 anti-GFP and blot with Invitrogen 33-2600 anti-GFP. Representative blot from three biological replicates.

Figure 5

Kinetics of dissociation of PI5P4Kγ dimers.

Untagged recombinant PI5P4Kγ was allowed to reach equilibrium at a concentration where dimers are the predominant species. The solution was then diluted to a concentration at which we would expect monomers to predominate and samples were taken with cross linking at the intervals shown. Detection with anti-PI5P4Kγ antibody [17] as specified in supplementary methods. Representative blot from three replicates.

Figure 6

Growth characteristics of PIP4K2B$^{-/-}$ cells.

A: WT DT40 and PIP4K2B$^{-/-}$ cells were allowed to grow into the death phase without replacement of growth medium. Although the rate of proliferation of the two cell lines is similar in the exponential phase, this phase lasts longer in PIP4K2B$^{-/-}$ cells resulting in these cells attaining a higher density in the stationary phase. Cell density was significantly higher for PIP4K2B$^{-/-}$ cells at all time points from 30 hours onwards, $P<0.001$. Data analysis by ANOVA. At each data point mean and 95% confidence interval is plotted. n=3 biological replicates.

B: Representative flow cytometry traces of cell cycle distribution corresponding to the growth curves in (A). Graph shows the percentage of cells in G1 at each time point. WT DT40 and PIP4K2B$^{-/-}$ cells grow similarly until 28 hours from which time PIP4K2B$^{-/-}$ cells show delayed arrest at the G1/S checkpoint. At 28 hours 56% of WT DT40 cells are in G1 (95%CI 44% to 67%) compared to 43% of PIP4K2B$^{-/-}$ cells (95%CI 32% to 54%, $P<0.05$). At 32 hours 72% of WT DT40 cells are in G1 (95%CI 59% to 85%) compared to 44% of PIP4K2B$^{-/-}$ cells (95%CI 33% to 56%, $P<0.001$). Bars show mean and 95% confidence interval. Data analysis by ANOVA. n=3 biological replicates.

Figure 7

Autophagy and mTORC1 activity in PIP4K2B$^{-/-}$ cells.

A: Figure shows a representative western blot and quantification of three such blots by densitometry. Results normalised to WT DT40 cells in the absence of bafilomycin. In the absence of bafilomycin PIP4K2B$^{-/-}$ cells have a LC3-II to beta actin ratio of 2.39 (95%CI 1.74 to 3.04, P<0.01, n=3 biological replicates). In the presence of bafilomycin PIP4K2B$^{-/-}$ cells maintain a higher LC3-II to beta actin ratio than WT DT40 cells (Mean 4.96, 95%CI 3.85 to 6.07 versus mean 2.39, 95%CI 1.74 to 3.04; P<0.001, n=3 biological replicates). Bars show mean and 95% confidence interval. Bafilomycin was used at 10nM and blocks flux through the autophagy pathway. Blots with Sigma AC74 anti-beta actin and Cell Signaling Technology #2775 anti-LC3B.

B: mTORC1 mediated phosphorylation of p70 S6 kinase in PIP4K2B$^{-/-}$, PIP4K2A$^{-/-/-}$ and WT DT40 cells. Figure shows a representative western blot and quantitation of three such blots by densitometry. Normalized to WT DT40 cells the phospho- to total p70 S6K ratio in PIP4K2B$^{-/-}$ cells is 0.49 (95%CI 0.31 to 0.66, P<0.001, n=3 biological replicates) and in PIP4K2A$^{-/-/-}$ cells is 1.03 (95%CI 0.80 to 1.25, P=0.64, n=3 biological replicates). Bars show mean and 95% confidence interval. Blots with Cell Signaling Technology #9202 anti-p70 S6K and Cell Signaling Technology #9234 anti-phospho-Thr389-p70 S6K.

Supplementary Methods

Constructs to endogenously tag *PIP4K2A* and *PIP4K2B* with EmGFP at the C-terminus

The constructs used to endogenously tag *PIP4K2A* and *PIP4K2B* with EmGFP at the C-terminus were built into the multiple cloning site of pBluescript SK+ (Stratagene). Constructs used for genomic targeting never need to be expressed off their plasmid vector and so pBluescript, a bacterial cloning vector, is suitable for this purpose. The general strategy for designing these constructs is described in the main methods section.

The 2kb 5' homology arm of the *PIP4K2A* tagging construct was PCR amplified from DT40 gDNA using primers 2A5FOR2 and 2A5REV2 and cloned into pBluescript SK+ between KpnI and XbaI sites. An unwanted BamHI site was removed from the 5' arm by site directed mutagenesis using primers SDM5 and SDM6. Next the coding sequence for EmGFP was PCR amplified from the plasmid EmGFP-C1 (primers EGFP_PCR_FOR_1 and EGFP_PCR_REV_1) and cloned into the construct between XbaI and BamHI sites. The 2kb 3' homology arm of the targeting construct was then cloned into the construct between BamHI and NotI sites following PCR amplification from DT40 gDNA (primers 2A3FOR2 and 2A3REV2). Finally either a puromycin resistance cassette or a blasticidin resistance cassette was ligated into the BamHI site of the construct following excision from the pLOX PURO or pLOX BSR plasmids respectively. Having two constructs identical save for the antibiotic resistance conferred allowed sequential targeting of two *PIP4K2A* alleles using different selection antibiotics in order to derive the cell line PIP4K2A$^{wt/EmGFP/EmGFP}$, which is resistant to both puromycin and blasticidin. Note that the antibiotic selection cassettes used contained their own eukaryotic promoters. Tagging two *PIP4K2A* alleles in DT40 cells leaves one wild type allele as DT40 cells exhibit trisomy for chromosome 2, the chromosome on which the *PIP4K2A* gene is located. The correct integration of each targeting construct was tested by long-range PCR and sequencing, and the presence of a third *PIP4K2A* allele was verified by the ability to PCR out a wild type region spanning the terminal *PIP4K2A* exon from PIP4K2A$^{wt/EmGFP/EmGFP}$ gDNA. In order to verify the correct expression of the PtdIns5P 4-kinase alpha – EmGFP fusion protein PIP4K2A$^{wt/EmGFP/EmGFP}$ cells were subjected to immunoprecipitation and western blotting with anti-GFP antibodies. A GFP-containing protein of the correct

molecular weight was present in PIP4K2A$^{wt/EmGFP/EmGFP}$ cells but not in WT DT40 cells. Importantly this 70KDa protein was the only GFP-containing species present in the tagged cells. These controls to ensure accurate construct integration and appropriate fusion protein expression were performed for every tagged cell line generated.

In the case of *PIP4K2B*, we could start from the construct we previously generated to tag PI5P4Kβ with FLAG-$(His)_6$ [15]. We excised the coding sequence for the FLAG-$(His)_6$ tag and ligated in the coding sequence for EmGFP. Once again two targeting constructs were made, identical save for the presence of either a puromycin or blasticidin resistance cassette. These constructs were used to sequentially target both alleles of *PIP4K2B* to render the cell line PIP4K2B$^{EmGFP/EmGFP}$.

Constructs to delete *PIP4K2A* and *PIP4K2B*

The 5' arm of the *PIP4K2A* deletion construct was amplified from DT40 gDNA using primers GGPIP4K2A_DEL_5'_FOR_2 and GGPIP4K2A_DEL_5'_REV_2 whilst the 3' arm was amplified using primers GGPIP4K2A_DEL_3'_FOR and GGPIP4K2A_DEL_3'_REV. These arms were ligated into pBluescript SK+ between KpnI and BamHI sites (5' arm) and BamHI and NotI sites (3' arm). A neomycin, puromycin, or blasticidin resistance cassette was then ligated into the BamHI site to generate three constructs that were used sequentially in order to delete all three PIP4K2A loci to generate PIP4K2A$^{-/-/-}$ cells.

The primer pairs used to amplify the 5' and 3' arms of the *PIP4K2B* deletion construct were 2b_Ful_Del_PCR_5'_For_1 and 2b_Ful_Del_PCR_5'_Rev_1, and 2b_Ful_Del_PCR_3'_For_1 and 2b_Ful_Del_PCR_3'_Rev_1 respectively. The two *PIP4K2B* loci in DT40 cells were sequentially deleted using puromycin and blasticidin resistance cassettes to derive the cell line PIP4K2B$^{-/-}$. In order to generate a cell line expressing EmGFP-tagged PI5P4Kα in a *PIP4K2B* null background a neomycin resistance cassette was ligated into the *PIP4K2A* targeting construct already described. This construct was then be used to target a *PIP4K2A* locus in PIP4K2B$^{-/-}$ cells to generate the cell line PIP4K2A$^{EmGFP/wt/wt}$PIP4K2B$^{-/-}$.

Tagging of *PIP4K2B* at the C-terminus with the auxin degron system

The coding sequence for osTIR1 (the part of the auxin degron system that needs to be stably expressed for the method to work) was PCR-amplified from the pNHK60 plasmid (kindly provided by Gerard Evan, Cambridge) using the primers PCR-osTIR1-F and R and subcloned into pcDNA3.1 between Ecor1 and Kpn1 restriction sites for stable transfection into DT40 cells. The DNA sequence encoding for an eight amino acid flexible linker followed by the AtIAA17 (degron) tag were PCR-amplified from the pNHK60 plasmid using the primers pBAIDII-1-F and R, and subcloned in frame with a C-terminal purification tag (a FLAG-$(His_6)_2$ tag) using a pBluescript SK+ derivative [15]. This construct was then excised between Sal1 and BamH1 restriction sites and subcloned in between 5' and 3' *PIP4K2B*-targeting homology arms as described above. Antibiotic selection markers were then cloned in as described above. Sequential targeting of the *PIP4K2B* loci with constructs conferring resistance to different antibiotics yielded the cell line $PIP4K2B^{degron/degron}$. Using a spare antibiotic selection cassette a *PIP4K2A* allele could then be targeted with an EmGFP tag as described above to give the cell line $PIP4K2A^{EmGFP/wt/wt}PIP4K2B^{degron/degron}$.

Antibodies

Target	Manufacturer and Product Number
6xHis tag	Abcam Ab9108.
Beta actin	Sigma Aldrich. AC74.
FLAG	Sigma Aldrich A2220.
Green fluorescent protein	Invitrogen 33-2600 raised in mouse for western blotting
Green fluorescent protein	Invitrogen A-6455 raised in rabbit for immunoprecipitation
Histone H3	Abcam ab1791.
LC3B	Cell Signaling Technology #2775.
Mouse IgG (H+L) peroxidase conjugated	Vector Laboratories PI-2000.
Total p70 S6K	Cell Signaling Technology #9202
Phospho-Thr389-p70 S6K	Cell Signaling Technology #9234
PI5P4Kγ	NeoMPS. Antibody raised in rabbit to a

	peptide corresponding to amino acids 333–352 of mouse PI5P4Kγ. See reference [17] in the main paper.
Rabbit IgG (H+L) peroxidase conjugated	Abcam ab16284.

Primers

Primer name	**Primer sequence (5' to 3')**
2A5FOR2	TTA AGG TAC CGA GCT GCT GAG TGA TCC TAA AG
2A5REV2	GCA TTC TAG ACG TCA AGA TGT TGG CAA TAA AG
SDM5	CAA GTA GGG ACA CAT TGC ATC CAA CTG CAG TAG TTC AG
SDM6	CTG AAC TAC TGC AGT TGG ATG CAA TGT GTC CCT ACT TG
EGFP_PCR_FOR_1	TCT TCA TCT AGA ATG GTG AGC AAG GGC GAG GAG
EGFP_PCR_REV_1	CAC CAG GGA TCC TTA CTT GTA CAG CTC GTC CAT GC
2A3FOR2	TAA TGG ATC CCC CCT CAT GTC ACA CCG GAC
2A3REV2	TCA TGC GGC CGC TGC TAC ACA GAC AGA AAG TG
GGPIP4K2A_DEL_5'_FOR_2	TGG TGG TAC CTA GTG GGA GGA CTT GCA AAT GAG G
GGPIP4K2A_DEL_5'_REV_2	ACC AGG ATC CAA TCA GGT GTC AGA CCA CTT CAC G
GGPIP4K2A_DEL_3'_FOR	TAT AGG ATC CTC TGT GGG TAG TGT GCT TAG GTG
GGPIP4K2A_DEL_3'_REV	ATT AGC GGC CGC CTG CCA GTC TGT CCA TCC TCT GA
2b_Ful_Del_PCR_5'_For_1	TCA AGG TAC CTG GAG AGC AGA TTG TCA CAC

2b_Ful_Del_PCR_5'_Rev_1	TGA CGG ATC CCA GAA AGA CAC ACA TAC ACA C
2b_Ful_Del_PCR_3'_For_1	TGC AGG ATC CGC TTC CCT CGT GCT AAG GAT TG
2b_Ful_Del_PCR_3'_Rev_1	TAA TGC GGC CGC GCT ACC TAC ATC CAG CAC AG
PCR-osTIR1-F	ATA TGA ATT CAT GAC GTA CTT CCC GGA GGA G
PCR-osTIR1-R	ATA TGG TAC CTT ACC ACT AGC AGC AGA ACC GGA G
pBAIDII-1-F	ATA TGT CGA CGG AGC TGG TGC AGG CG
pBAIDII-1-R	ATA TTC TAG AAG CTC TGC TCT TGC ACT T

Supplementary Results and Discussion

It is important to establish that the various endogenous tags we have introduced into the PI5P4Ks do not in themselves affect protein expression or function. Unfortunately given the low expression of PI5P4Kα and PI5P4Kβ in DT40 cells, and the lack of isoform selective antibodies with which to investigate these enzymes, we cannot directly compare protein expression levels in tagged versus untagged cells. We can, however, investigate expression at the mRNA level by qPCR and find that the presence of endogenous EmGFP coding sequences does not affect this read-out of expression (supplementary figure 1A). We can also establish, by pulling down and blotting against the EmGFP tag, that the presence of the tag does not result in protein degradation; the only EmGFP-containing species detected in tagged cell lines is of the correct size for the full-length fusion protein (see supplementary figure 1B for an example in PIP4K2A$^{EmGFP/EmGFP/wt}$ cells). Most importantly, we can establish that phenotypic changes seen upon gene deletion do not occur in tagged cells, and therefore the tagged protein must be functioning normally at least as far as the phenotype studies is concerned. PIP4K2B null cells exhibit reduced p70 S6K phosphorylation at Thr389, but this phenotype is not observed in PIP4K2B$^{EmGFP/EmGFP}$ cells (supplementary figure 1C). The current manuscript is concerned principally with PI5P4Kβ, but we have data elsewhere that show the same principle to be true in cells where all three alleles of PI5P4Kα are tagged endogenously with EmGFP (Bulley, Droubi *et al.,* in submission). In degron-tagged cell lines the question does not arise, as throughout this manuscript we have shown phenotypes to emerge only when the PI5P4K-degron fusion protein is removed with auxin addition.

Supplementary Figure Legends

Supplementary Figure 1

A: In PIP4K2A$^{EmGFP/EmGFP/wt}$ cells the relative abundance of *PIP4K2A* mRNA compared to WT DT40 cells is 0.94 (95%CI 0.86 to 1.01) whilst the abundance of *PIP4K2B* mRNA is 0.91 (95%CI 0.84 to 0.97). In PIP4K2B$^{EmGFP/EmGFP}$ cells the relative abundance of *PIP4K2B* mRNA compared to WT DT40 cells is 1.01 (95%CI 0.96 to 1.06) whilst the abundance of *PIP4K2A* mRNA is 1.10 (95%CI 1.02 to 1.17). Bars show mean and 95% CI. n=3 biological replicates in all cases.

B: Immunoprecipitation and western blotting of EmGFP-containing species from WT

DT40 cells and PIP4K2A$^{EmGFP/EmGFP/wt}$ cells. Immunoprecipitation with Invitrogen A-6455 anti-GFP and blot with Invitrogen 33-2600 anti-GFP.

C: The phosphorylation status of p70 S6K at Thr389 in WT DT40, PIP4K2B$^{EmGFP/EmGFP}$, and PIP4K2B$^{-/-}$ cells. Blots with Cell Signaling Technology #9202 anti-p70 S6K and Cell Signaling Technology #9234 anti-phospho-Thr389-p70 S6K. Representative image from three replicates.

Figure 1

A

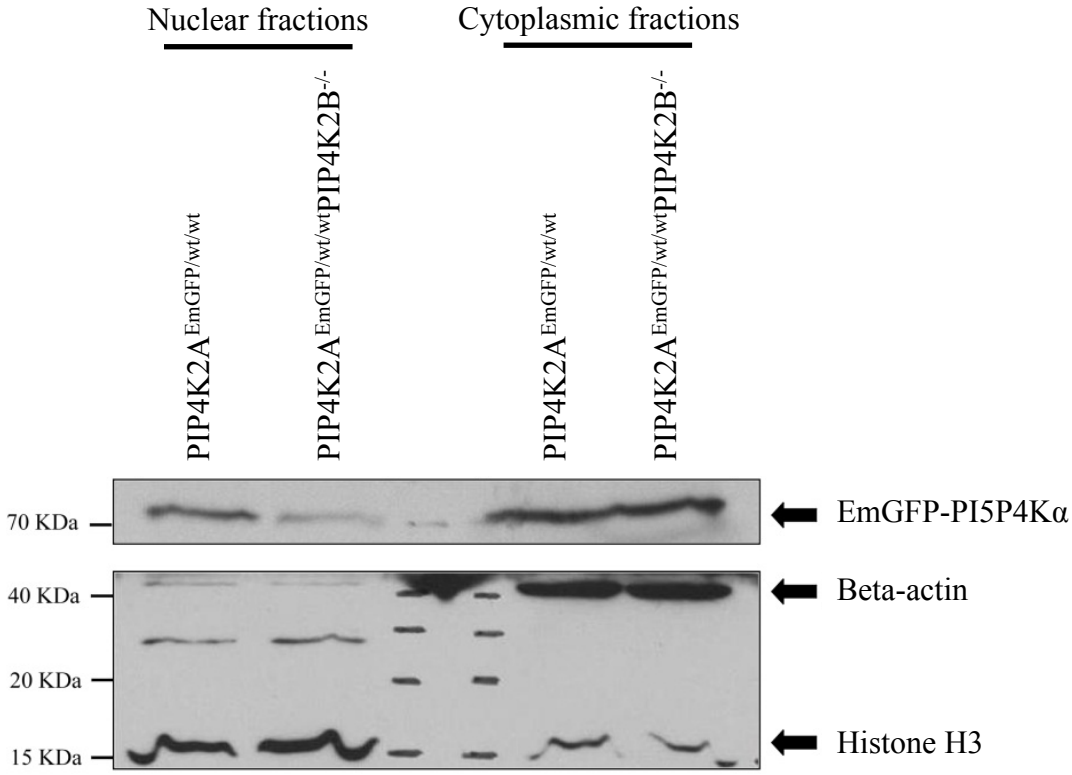
Nuclear fractions
Cytoplasmic fractions
PIP4K2A EmGFP/wt/wt
PIP4K2A EmGFP/wt/wt PIP4K2B -/-
PIP4K2A EmGFP/wt/wt
PIP4K2A EmGFP/wt/wt PIP4K2B -/-
70 KDa
40 KDa
20 KDa
15 KDa
EmGFP-PI5P4Kα
Beta-actin
Histone H3

B

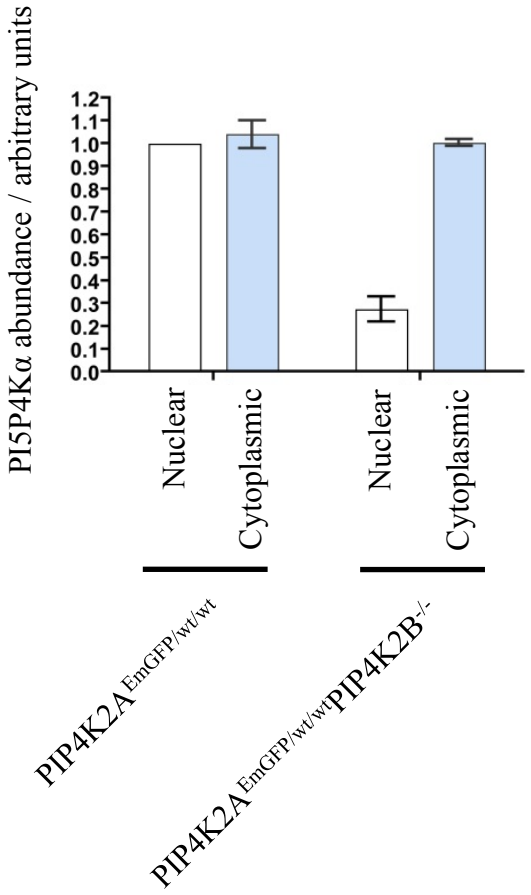
PI5P4Kα abundance / arbitrary units
1.2
1.1
1.0
0.9
0.8
0.7
0.6
0.5
0.4
0.3
0.2
0.1
0.0
Nuclear
Cytoplasmic
Nuclear
Cytoplasmic
PIP4K2A EmGFP/wt/wt
PIP4K2A EmGFP/wt/wt PIP4K2B -/-

Figure 2

A

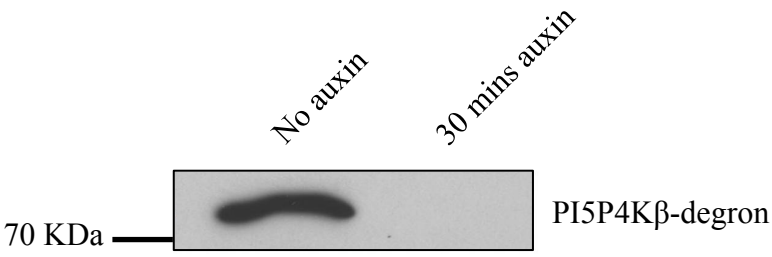
No auxin
30 mins auxin
70 KDa
PI5P4Kβ-degron

B

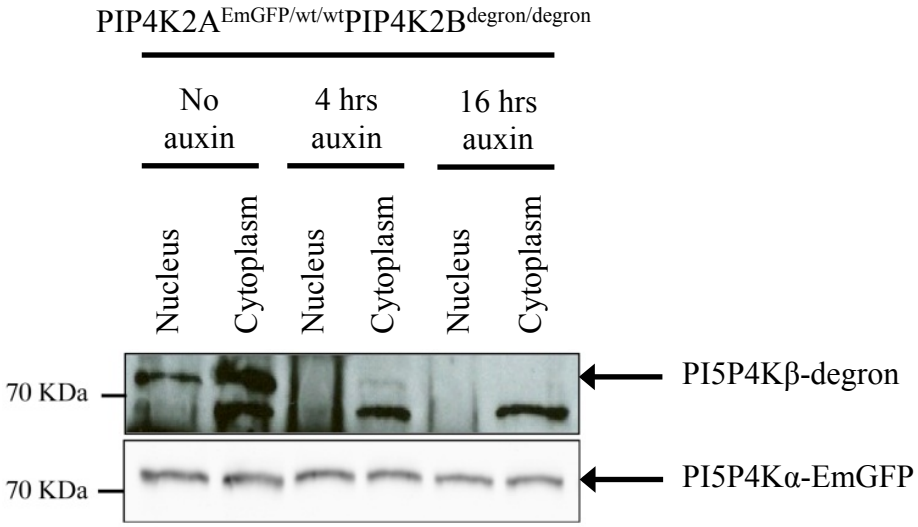
PIP4K2A EmGFP/wt/wt PIP4K2B degron/degron
No auxin
4 hrs auxin
16 hrs auxin
Nucleus
Cytoplasm
Nucleus
Cytoplasm
Nucleus
Cytoplasm
70 KDa
PI5P4Kβ-degron
70 KDa
PI5P4Kα-EmGFP

Figure 3

A

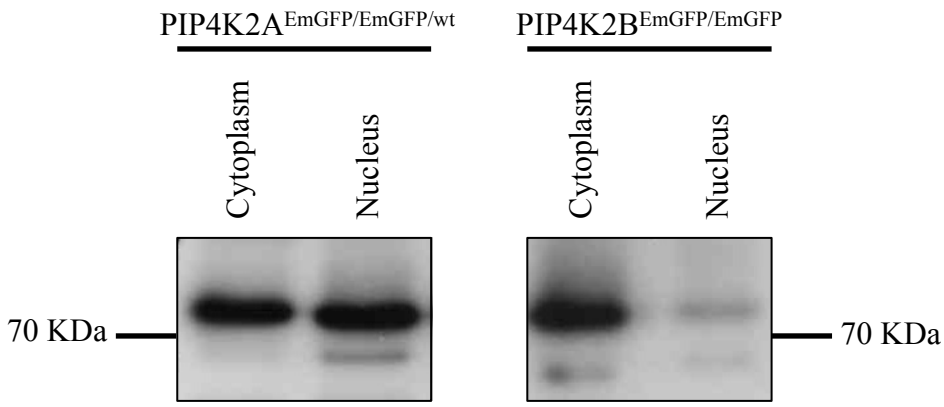
PIP4K2A EmGFP/EmGFP/wt
PIP4K2B EmGFP/EmGFP
Cytoplasm
Nucleus
Cytoplasm
Nucleus
70 KDa
70 KDa

B

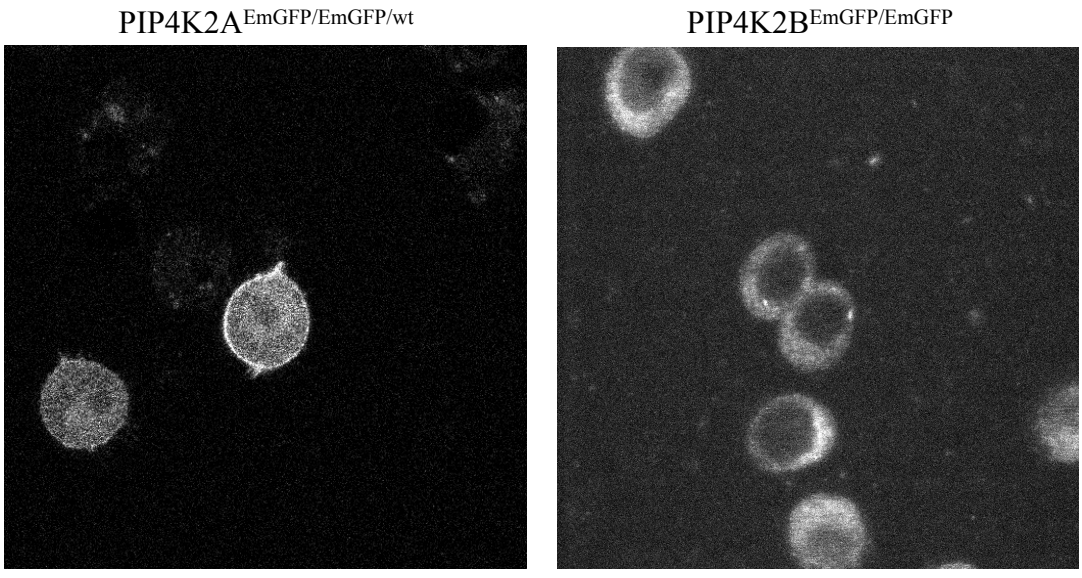
PIP4K2A EmGFP/EmGFP/wt
PIP4K2B EmGFP/EmGFP

Figure 4

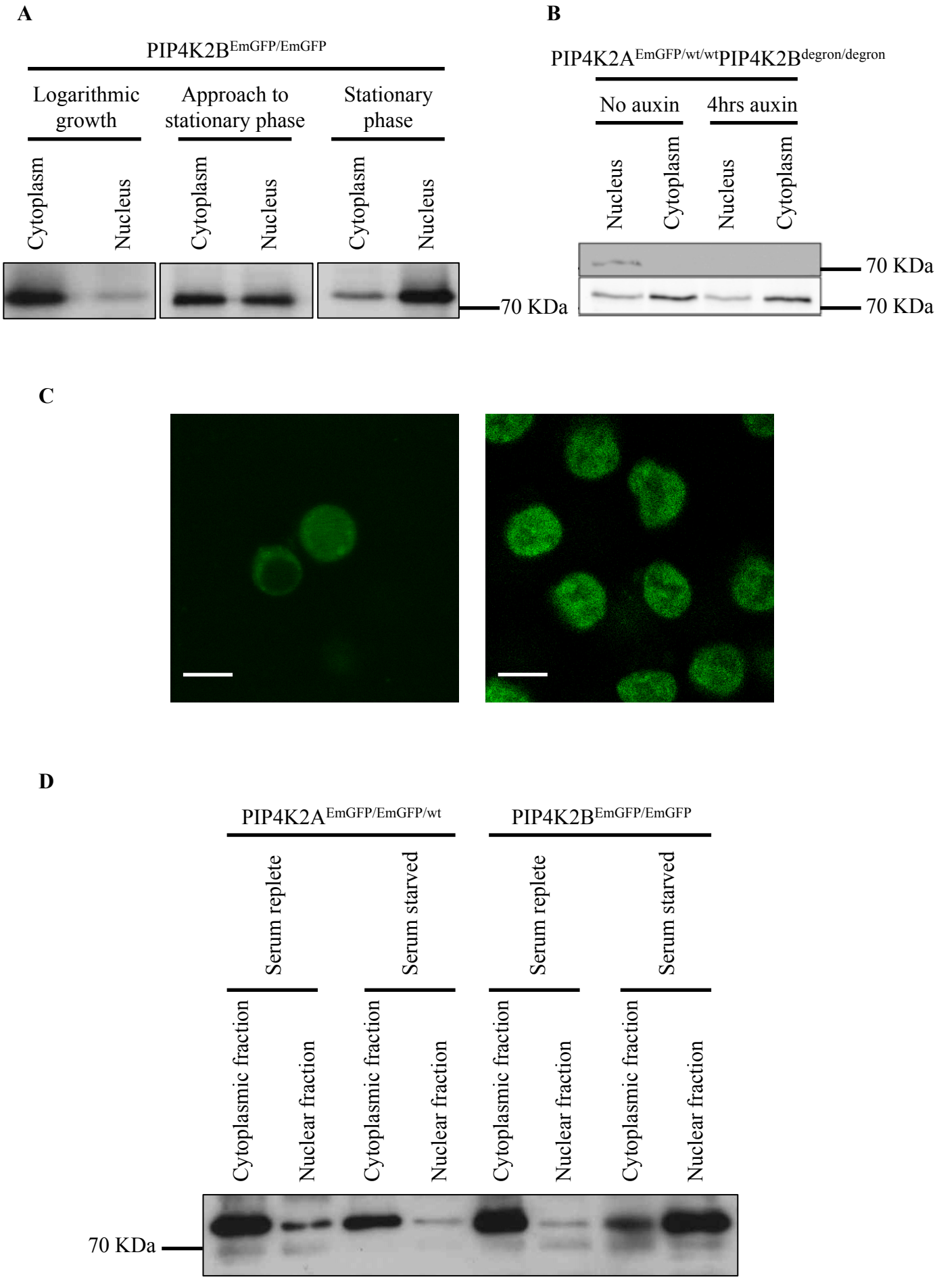
A
PIP4K2B EmGFP/EmGFP
Logarithmic growth
Approach to stationary phase
Stationary phase
Cytoplasm
Nucleus
Cytoplasm
Nucleus
Cytoplasm
Nucleus
70 KDa
B
PIP4K2A EmGFP/wt/wt PIP4K2B degron/degron
No auxin
4hrs auxin
Nucleus
Cytoplasm
Nucleus
Cytoplasm
70 KDa
70 KDa
C
D
PIP4K2A EmGFP/EmGFP/wt
PIP4K2B EmGFP/EmGFP
Serum replete
Serum starved
Serum replete
Serum starved
Cytoplasmic fraction
Nuclear fraction
Cytoplasmic fraction
Nuclear fraction
Cytoplasmic fraction
Nuclear fraction
Cytoplasmic fraction
Nuclear fraction
70 KDa

Figure 5

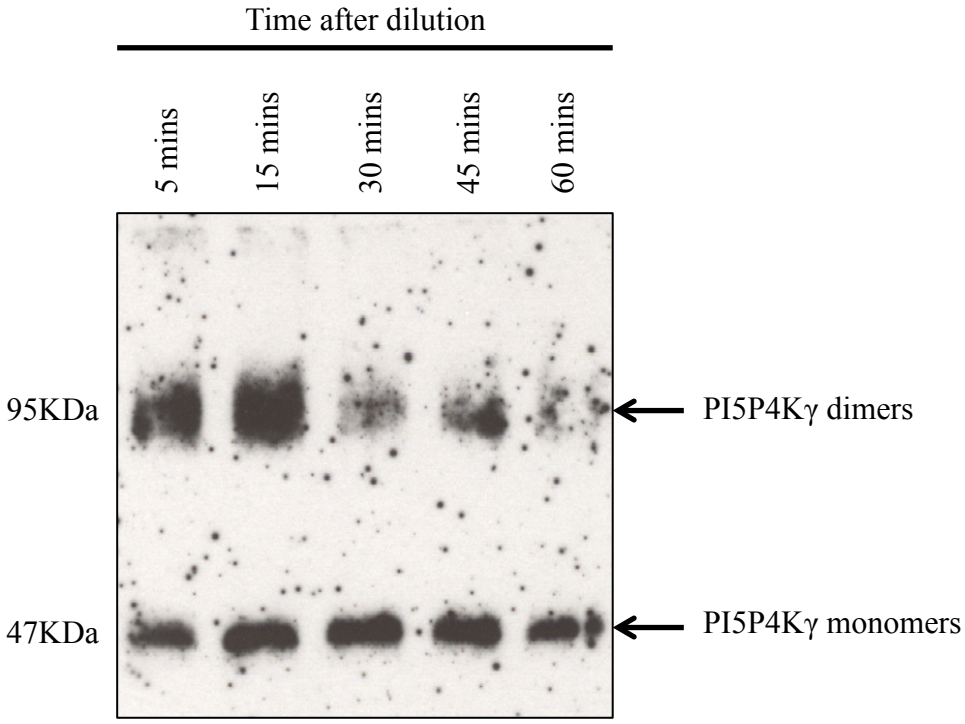
Time after dilution
5 mins
15 mins
30 mins
45 mins
60 mins
95KDa
47KDa
PI5P4Kγ dimers
PI5P4Kγ monomers

Figure 6

A

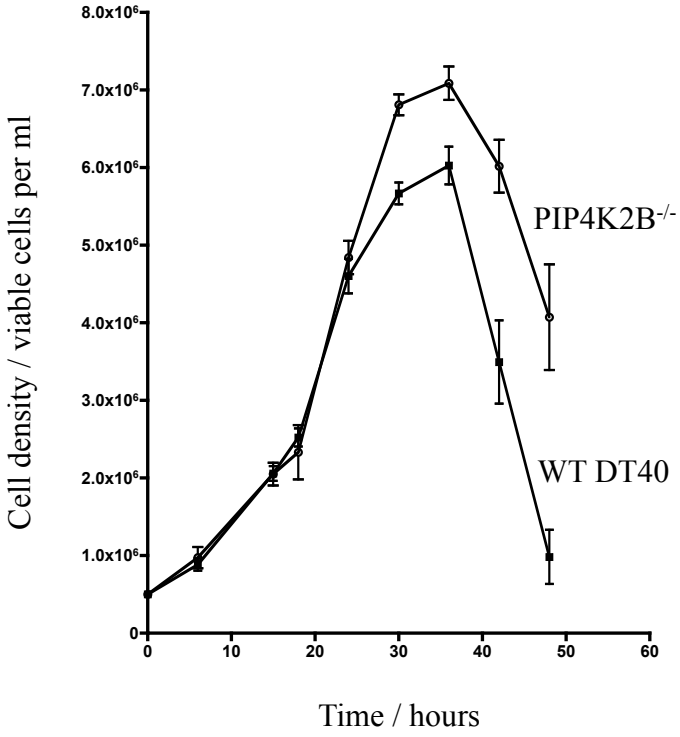
8.0x10⁶
7.0x10⁶
6.0x10⁶
5.0x10⁶
4.0x10⁶
3.0x10⁶
2.0x10⁶
1.0x10⁶
0
Cell density / viable cells per ml
PIP4K2B-/-
WT DT40
0
10
20
30
40
50
60
Time / hours

B

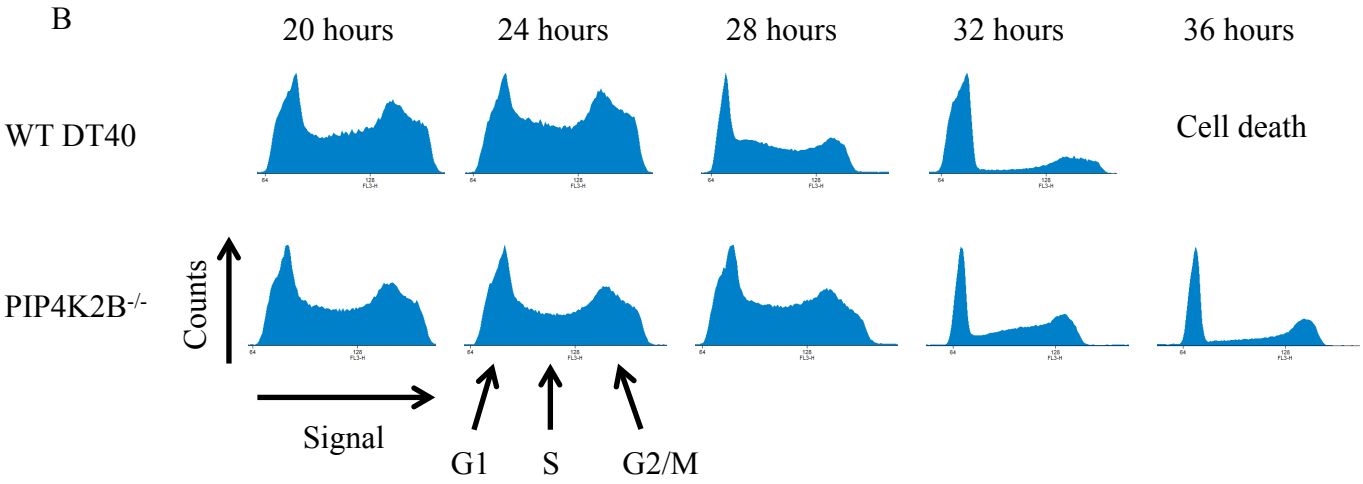
20 hours
24 hours
28 hours
32 hours
36 hours
WT DT40
Cell death
PIP4K2B-/-
Counts
Signal
G1
S
G2/M

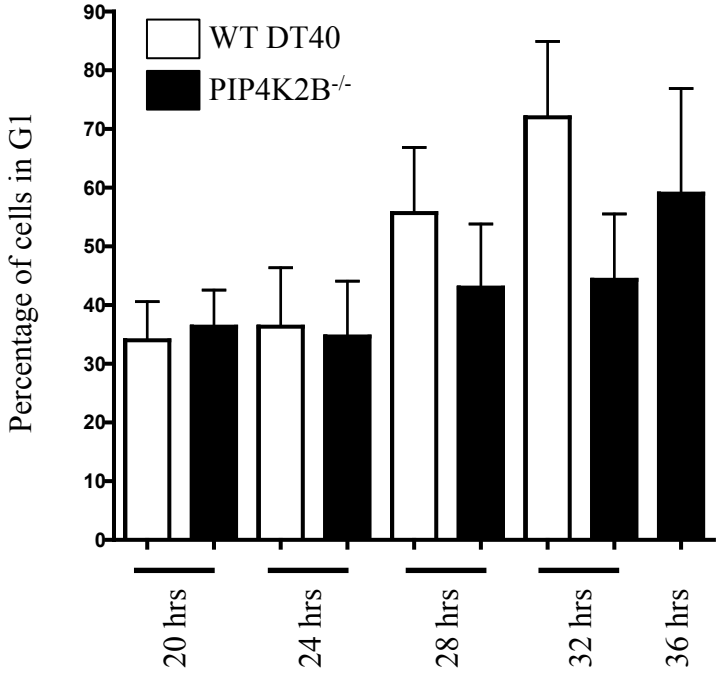
WT DT40
PIP4K2B-/-
Percentage of cells in G1
90
80
70
60
50
40
30
20
10
0
20 hrs
24 hrs
28 hrs
32 hrs
36 hrs

Figure 7

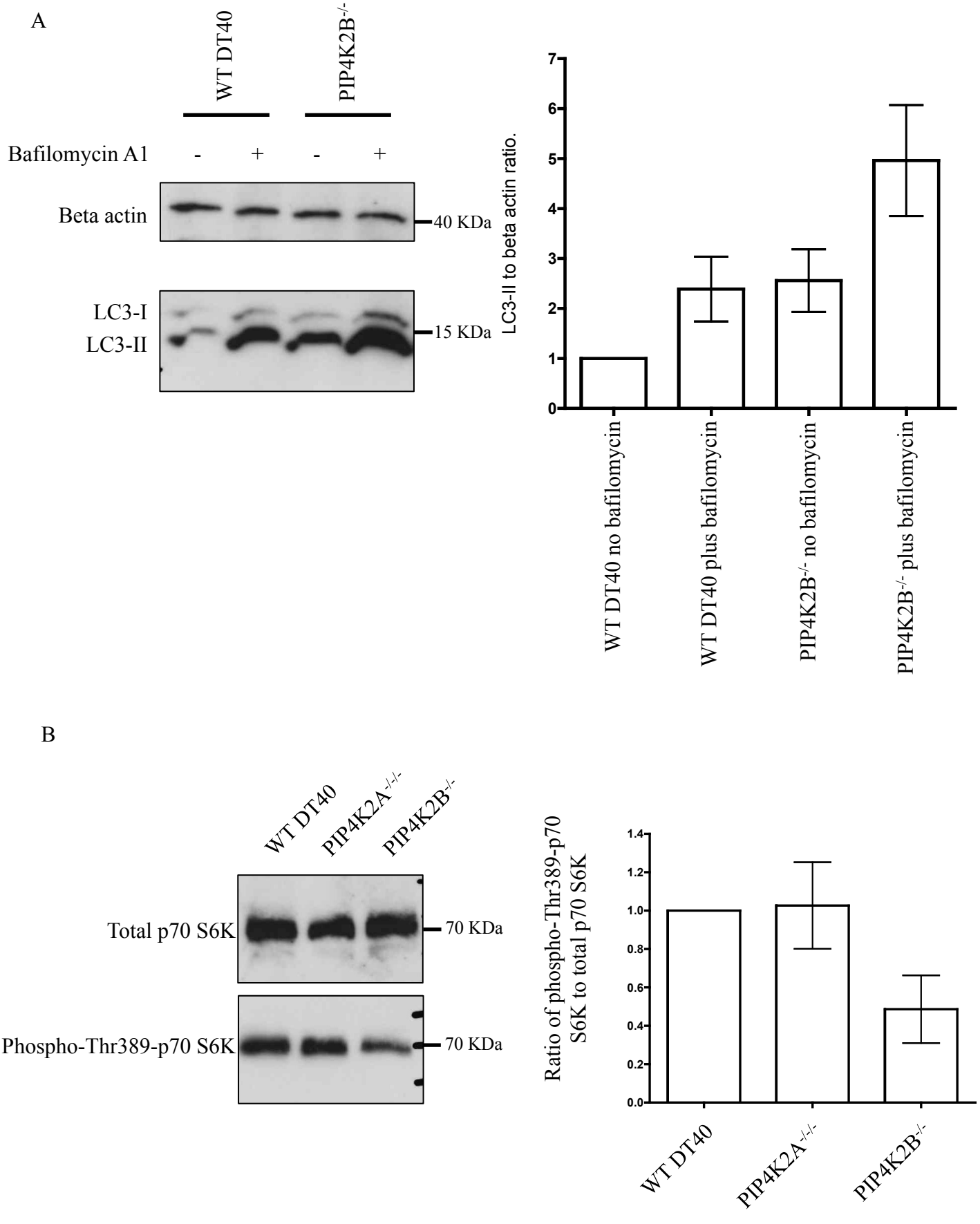
A
WT DT40
PIP4K2B-/-
Bafilomycin A1
- + - +
Beta actin
40 KDa
LC3-I
LC3-II
15 KDa
LC3-II to beta actin ratio.
0
1
2
3
4
5
6
7
WT DT40 no bafilomycin
WT DT40 plus bafilomycin
PIP4K2B-/- no bafilomycin
PIP4K2B-/- plus bafilomycin
B
WT DT40
PIP4K2A-/-
PIP4K2B-/-
Total p70 S6K
70 KDa
Phospho-Thr389-p70 S6K
70 KDa
Ratio of phospho-Thr389-p70 S6K to total p70 S6K
0.0
0.2
0.4
0.6
0.8
1.0
1.2
1.4
WT DT40
PIP4K2A-/-
PIP4K2B-/-

Figure S1

A

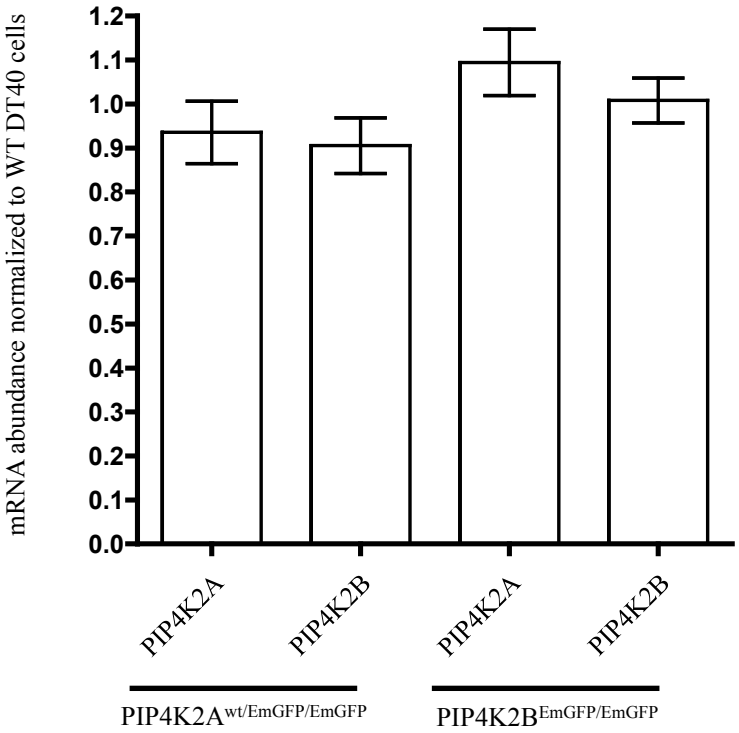

B

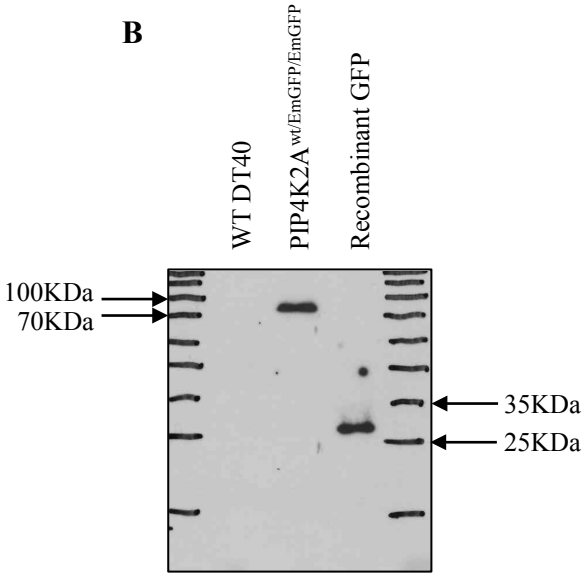

C